ORGANIC LETTERS

2006
Vol. 8, No. 8
1601−1604

Fluorescent Ratiometry of Tetrahomodioxacalix[4]arene Pyrenylamides upon Cation Complexation

Jung Kyu Choi,[†] Areum Lee,[‡] Seyoung Kim,[‡] Sihyun Ham,*[,‡] Kwanghyun No,*[,‡] and Jong Seung Kim*[,†]

Department of Chemistry, Institute of Nanosensor & Biotechnology, Dankook University, Seoul 140-714, Korea, and Department of Chemistry, Sookmyung Women's University, Seoul 140-742, Korea.

jongskim@dankook.ac.kr

Received January 27, 2006 *(Revised Manuscript Received February 27, 2006)*

ABSTRACT

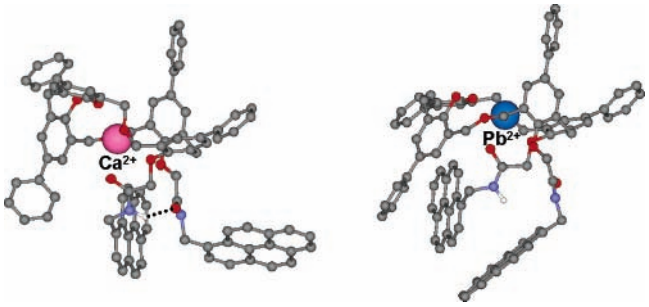

C-1,2-alternate tetrahomodioxacalix[4]arene pyreneamides were synthesized. Pb^{2+} coordination gave a quenched monomer and excimer fluorescence emission, while upon Ca^{2+} ion binding, the receptor provides an enhanced excimer and declined monomer emission with ratiometric response. The excimer emission spectra changes are rationalized by frontier molecular orbitals that the effective Py–Py* interaction induces emission intensity increases upon Ca^{2+} ion complexation, whereas there is no such interaction observed upon Pb^{2+} binding.

Optical signals based on the changes of absorbance or fluorescence have been focused on in many industrial fields including chemistry, biology, and medicine.[1,2] Most of the fluorescent chemosensors for cations are composed of a cation recognition unit (ionophore) together with a fluorogenic unit (fluorophore) and are called fluoroiono-phores.[3−5] As fluorogenic units, pyrenes (Py) are one of the most useful sensing probes due to their relatively efficient excimer formation and emission.[4] Since the intensity ratio of the excimer to the monomer emission (I_E/I_M) is sensitive to conformational changes of the pyrene-appended receptors, changes in I_E/I_M upon metal ion complexation can be an informative parameter in various sensing systems.[1,5−8] Recently, we reported that 1,3-alternate calix[4]crown-5 having two pyrenyl arms shows the excimer fluorescence quenched by Pb^{2+}, but revived by addition of K^+, which was evidenced

[†] Dankook University.
[‡] Sookmyung Women's University.

(1) de Silva, A. P.; Gunaratne, H. Q. N.; Gunnlaugsson, T.; Huxley, A. J. M.; McCoy, C. P.; Rademacher, J. T.; Rice, T. E. *Chem. Rev.* **1997**, *97*, 1515.
(2) *Chemosensors of Ion and Molecule Recognition*; Desvergne, J.-P., Czarnik, A. W., Eds.; NATO ASI Series; Kluwer Academic: Dordrecht, 1997; p 492.
(3) Valeur, B.; Leray, I. *Coord. Chem. Rev.* **2000**, *205*, 3.
(4) Fabbrizzi, L.; Poggi, A. *Chem. Soc. Rev.* **1995**, *24*, 197.
(5) (a) Nohta, H.; Satozono, H.; Koiso, K.; Yoshida, H.; Ishida, J.; Yamaguchi, M. *Anal. Chem.* **2000**, *72*, 4199. (b) Okamoto, A.; Ichiba, T.; Saito, I. *J. Am. Chem. Soc.* **2004**, *126*, 8364.
(6) Birks, J. B. *Photophysics of Aromatic Molecules*; Wiley-Interscience: London, 1970.
(7) Winnik, F. M. *Chem. Rev.* **1993**, *93*, 587.
(8) (a) Lewis, F. D.; Zhang, Y.; Letsinger, R. L. *J. Am. Chem. Soc.* **1997**, *119*, 5451. (b) Lou, J.; Hatton, T. A.; Laibinis, P. E. *Anal. Chem.* **1997**, *69*, 9, 1262. (c) Reis e Sousa, A. T.; Castanheira, E. M. S.; Fedorov, A. Martinho, J. M. G. *J. Phys. Chem. A* **1998**, *102*, 6406. (d) Suzuki, Y.; Morozumi, T.; Nakamura, H.; Shimomura, M.; Hayashita, T.; Bartsch, R. A. *J. Phys. Chem. B* **1998**, *102*, 7910.

10.1021/ol0602396 CCC: $33.50
Published on Web 03/16/2006

by computational results that HOMO−LUMO interactions are absent in the Pb^{2+} complex.[9]

Homooxacalix[4]arenes containing extra oxygen atoms in the macrocyclic array have received much attention because of their flexibility in solution.[10−14] We reported that C-1,2-alternate tetrahomodioxacalix[4]arene tetraamide selectively encapsulates Pb^{2+} over other metal ions with formation of a 1:1 complex.[13,14]

Focusing on the complexation selectivity following the fluorescence changes, we herein report for the first time on the series of C-1,2-alternate tetrahomodioxa-*p*-phenylcalix-[4]arenes (**1** and **2** in Figure 1), synthesis (Scheme S1 in

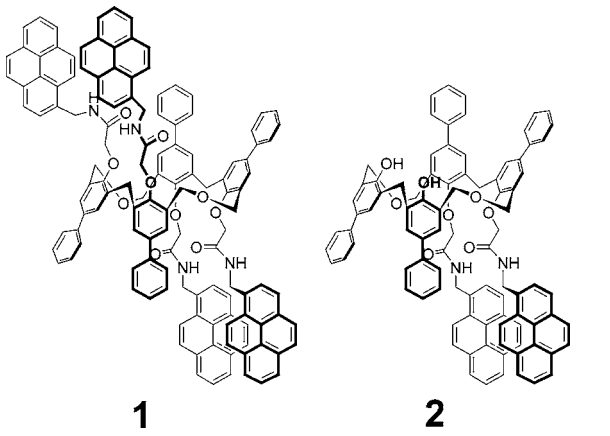

Figure 1. Structure of fluorescence chemosensors **1** and **2**.

Supporting Information), and their pyrene monomer and excimer emission changes upon metal ion complexation as well as the thermodynamic stability of the complex based on the theoretical calculation.

Compound **1** was synthesized by the reaction of tetrahomodioxacalix[4]arene (**3**)[13] with excess (1-pyrenemethyl)chloroacetamide (**4**)[12] in the presence of a catalytic amount of NaI and excess K_2CO_3 as a base as shown in Scheme S1. Compound **2** was also synthesized by the reaction of **3** with 2.1 equiv of **4** in the presence of catalytic amount of NaI and 2.1 equiv of K_2CO_3 as a base. Both **1** and **2** were found to be in C-1,2-alternate conformation of which the nomenclature was previously designated by our research group[13,14] by ^1H and ^{13}C NMR spectrum.

As seen in Figure 2, both **1** and **2** show selectively decreasing fluorescence for the Pb^{2+} over other metal ions. When the Pb^{2+} ion is coordinated to the two carbonyl groups

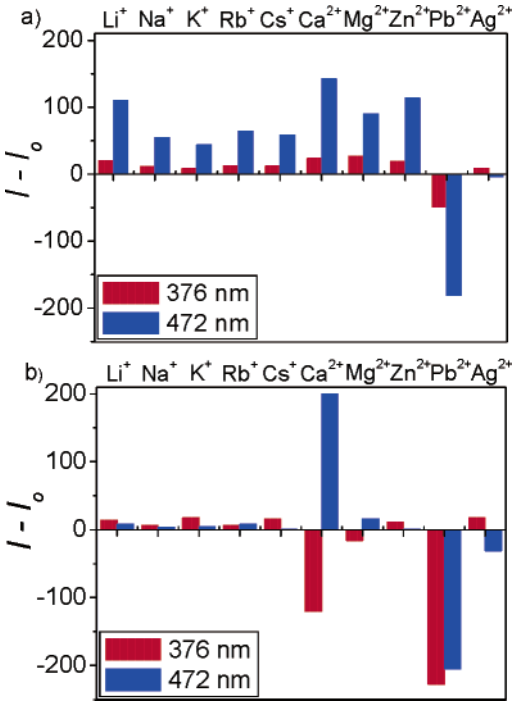

Figure 2. Fluorescence changes ($I - I_o$) of **1** (a) and **2** (b) upon addition of various metal ions. Conditions: **1** and **2** (6.0 μM) in $CHCl_3/CH_3CN$ (1:3, v/v), excitation at 343 nm, metal perchlorate (500 equiv) in $CHCl_3/CH_3CN$ (1:3, v/v). *I*: fluorescence emission intensity of complexes **1** and **2**. I_o: fluorescence emission intensity of free **1** and **2**.

of the amides of **1** or **2**, the carbonyl groups containing two pyrene units change the conformation,[15] which induces the disruption of the neighboring Py−Py* interaction (see the calculation part below). In addition, for the reducing mononer emission, a reverse-PET (photoinduced electron transfer)[16,17] and a heavy metal ion effect[18] of the Pb^{2+} ion are mainly considered (Figure S1 in Supporting Information).

Unlike **1**, receptor **2** bearing only a pair of pyrenes and two intact OHs on the lower rim reveals the sensitivity for both Pb^{2+} and Ca^{2+} ions as shown in bar profiles of Figure 2. Upon the addition of Pb^{2+} ion, the monomer and excimer emissions of **2** are quenched much more than the case of **1**. This is probably because the receptor **1** forms a 1:1 complex with metal ion in the solution as evidenced by the Job plot experiment (Figure S2 in Supporting Information); hence, the other pair of pyrenes of **1** is still active to provide an eminent excimer emission. On the other hand, in the case of Ca^{2+} addition to a solution of **2**, we observed an increasing excimer emission and a concomitantly declining monomer emission with an isosbestic point centered at 431 nm as

(9) Kim, S. K.; Lee, S. H.; Lee, J. Y.; Bartsch, R. A. Kim, J. S. *J. Am. Chem. Soc*. **2004**, *126*, 16499.
(10) (a) Gutsche, C. D.; Dhawan, B.; No, K. H.; Muthukrishnan, R. *J. Am. Chem. Soc*. **1981**, *103*, 3782. (b) Masci, B.; Saccheo, S. *Tetrahedron Lett.* **1993**, *34*, 6635.
(11) Dhawan, B.; Gutsche, C. D. *J. Org. Chem*. **1983**, *48*, 1536.
(12) Marcos, P. M.; Ascenso, J. R.; Lamartine, R.; Pereira, J. L. C. *Tetrahedron* **1997**, *53*, 11791.
(13) No, K.; Lee, J. H.; Yang, S. H. Kim, M. J.; Kim, J. S. *J. Org. Chem.* **2002**, *67*, 3165.
(14) No, K.; Kim, J. S.; Shon, O. J.; Yang, S. H.; Suh, I. H.; Kim, J. G.; Bartsch, R. A.; Kim, J. Y. *J. Org. Chem.* **2001**, *66*, 5976.
(15) van der Veen, N. J.; Flink, S.; Deij, M. A.; Egberink, R. J. M.; van Veggei, F. C. J. M.; Reinhoudt, D. N. *J. Am. Chem. Soc.* **2000**, *122*, 6112.
(16) Ojida, A.; Mito-oka, Y.; Inoue, M.-A.; Hamachi, I. *J. Am. Chem. Soc*. **2002**, *124*, 6256.
(17) de Silva, A. P.; Gunarante, H. Q. N.; Lynch, P. M. L. *J. Chem. Soc., Perkin Trans.* **1995**, *2*, 685.
(18) Chae, M.-Y.; Cherian, X. M.; Czarnik, A. W. *J. Org. Chem.* **1993**, *58*, 5797.

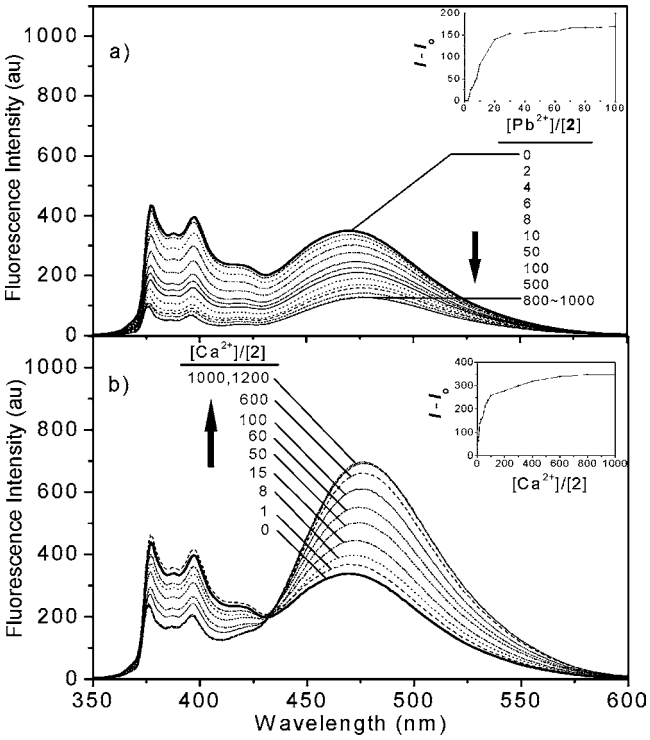

Figure 3. Fluorescence changes in emission spectra of **2** (6.0 μM) in $CHCl_3/CH_3CN$ (1:3, v/v) upon addition of Pb^{2+} (a) and Ca^{2+} (b). The inset shows the normalized intensity changes at 472 nm. The excitation wavelength is 343 nm.

shown in Figure 3. It is conceivable that the two facing phenol groups and amide oxygen atoms take part in the complexation of Ca^{2+}, which might allow the two pyrenes of **2** to locate more closely in the excited state so as to give a more stable Py−Py* interaction (vide infra), exerting an allosteric effect. The association constants (K_a)[19] of **2** for the Ca^{2+} were calculated to be 5.2×10^5 M^{-1}.

To understand the fluorescence intensity changes upon complexation, the density functional theory (DFT) calculations were employed for each host and its complex. An initial conformational analysis for each system was first performed by molecular dynamic (MD) simulation.[20] Then, we performed the geometry optimizations for each molecular system using the AM1 semiempirical method[21] to find the energy minima that would be used as initial structures for the DFT calculations at the B3LYP/3-21G* level[22] using the *Gaussian 98* package.[23]

The optimized geometries at the B3LYP/3-21G* level for **1** and **2** are represented in Figure S6 (Supporting Information). The lowest-energy conformation located at this level for both **1** and **2** is computed to be the C-1,2-alternate conformation, which is in agreement with the NMR assignment. The most distinctive structural feature for the conformational preference is the relative orientation of the adjacent pyrene amide groups. The preferential geometries for free polycyclic aromatic hydrocarbon (PAH) are displayed in two forms: One corresponds to a stacked structure favored by the dispersion interaction, and the other is a T-shaped (edge-on) structure employed by the electrostatic interaction.[24] Neither cases were applied to both **1** and **2**. The preferred geometry for each host is to allow NH···OC hydrogen bonding between the two amide groups linked to pyrene, rendering the neighboring pyrene groups almost in-plane. The NH···OC hydrogen bond distances in both **1** and **2** are found to be 1.90 Å.

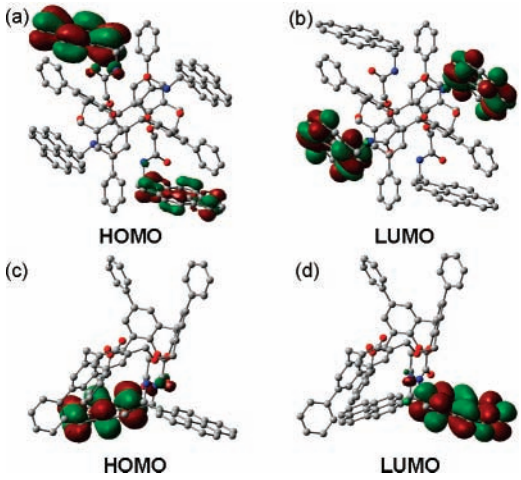

Figure 4. HOMO and LUMO for **1** and **2** are shown. (a) HOMO of **1**, (b) LUMO of **1**, (c) HOMO of **2**, and (d) LUMO of **2**.

For the investigations of fluorescence behavior, the Hückel molecular orbital calculations were performed at the B3LYP/3-21G* level. The highest occupied molecular orbital (HOMO) and lowest unoccupied molecular orbital (LUMO) for **1** are shown in (a) and (b), and those for **2** are in (c) and (d), respectively, in Figure 4. It was found that most of the electron densities in the HOMO are localized in one pyrene, and the LUMO is localized in the neighboring pyrene. On

(19) The computer program ENZFITTER, available from Elsevier-BIOSOFT, 68 Hills Road, Cambridge CB2 1LA, United Kingdom. (b) Connors, K. A. *Binding Constants*; Wiley: New York, 1987.

(20) Case, D. A.; Pearlman, D. A.; Caldwell, J. W. *AMBER 7*; University of California: San Francisco, 2002.

(21) (a) Dewar, M.; Thiel, W. *J. Am. Chem. Soc.* **1977**, *99*, 4499. (b) Dewar, M.; Zoebisch, E. G.; Healy, E. F. *J. Am. Chem. Soc.* **1985**, *107*, 3902.

(22) Becke, A. D. *J. Chem. Phys.* **1993**, *98*, 5648.

(23) Frisch, M. J.; Trucks, G. W.; Schlegel, H. B.; Scuseria, G. E.; Robb, M. A.; Cheeseman, J. R.; Zakrzewski, V. G.; Montgomery, J. A., Jr.; Stratmann, R. E.; Burant, J. C.; Dapprich, S.; Millam, J. M.; Daniels, A. D.; Kudin, K. N.; Strain, M. C.; Farkas, O.; Tomasi, J.; Barone, V.; Cossi, M.; Cammi, R.; Mennucci, B.; Pomelli, C.; Adamo, C.; Clifford, S.; Ochterski, J.; Petersson, G. A.; Ayala, P. Y.; Cui, Q.; Morokuma, K.; Malick, D. K.; Rabuck, A. D.; Raghavachari, K.; Foresman, J. B.; Cioslowski, J.; Ortiz, J. V.; Stefanov, B. B.; Liu, G.; Liashenko, A.; Piskorz, P.; Komaromi, I.; Gomperts, R.; Martin, R. L.; Fox, D. J.; Keith, T.; Al-Laham, M. A.; Peng, C. Y.; Nanayakkara, A.; Gonzalez, C.; Challacombe, M.; Gill, P. M. W.; Johnson, B. G.; Chen, W.; Wong, M. W.; Andres, J. L.; Head-Gordon, M.; Replogle, E. S.; Pople, J. A. *Gaussian 98*, revision A.7; Gaussian, Inc.: Pittsburgh, PA, 1998.

(24) Sahoo, D.; Narayanaswami, V.; Kay, C. M.; Ryan, R. O. *Biochemistry* **2000**, *39*, 6594.

the basis of the molecular orbital calculations, the HOMO−LUMO interactions between ground-state and excited-state pyrenes (Py−Py*) presumably contribute to the strong fluorescence excimer bands in both **1** and **2**.

To understand the nature of the fluorescence spectral change of the chemosensors upon the metal complexation, we also performed the geometry optimizations for **2**·Ca^{2+} and **2**·Pb^{2+} complexes (Figure 5). For both metal ions, the most significant difference upon complexation is the nucleation of the binding sites (all possible oxygen atoms) to maximize the electrostatic interactions between oxygen atoms and metal ion in that the cavities are fairly distorted and benzene rings are tilted away from the cavity. It is noticeable that the oxygen atoms in the −COC− bridges of the cavity are participating to recognize the metal ion, confirming that the homooxacalixarene provides extra binding sites compared to the analogous calixarene. For the **2**·Ca^{2+} complex (Figure 5a), the NH···OC hydrogen bonding (1.94 Å) between the two amide groups is still active, albeit the relative orientation of pyrenyl amide groups is somwhat changed to maximize the extent of the electrostatic interactions between O and Ca^{2+}. On the other hand, in the case of the **2**·Pb^{2+} complex (Figure 5b), the NH···OC hydrogen bonding is compensated to maximize electrostatic interactions between Pb^{2+} and oxygen atoms in the host. It is noted that the binding energy for **2**·Pb^{2+} is computed to be larger than that for **2**·Ca^{2+} by 20 kcal/mol.

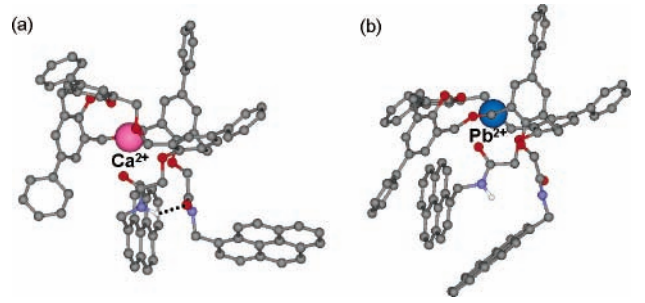

Figure 5. Calculated geometries (B3LYP/3-21G*) for (a) **2**·Ca^{2+} and (b) **2**·Pb^{2+}. Hydrogen atoms are omitted for clarity, except the hydrogen in NH···OC bonding. In the **2**·Ca^{2+} complex, the hydrogen bonding between amides is shown in the dotted line. Oxygen atoms are shown in red; nitrogen atoms are in blue.

The frontier molecular orbital calculations were executed for **2**·Ca^{2+} and **2**·Pb^{2+} complexes. In Figure 6a and b, the HOMO and LUMO for **2**·Ca^{2+} are localized on the pyrene units as in the case of the free host. On the other hand, in Figure 6c and d, the coordination of Pb^{2+} perturbs the electron density profile significantly so that none of LUMO, LUMO2, and LUMO3 are associated with pyrene. From the electron density analyses of the molecular orbitals, strong excimer emission can be explained by the stabilization of the excited state by Py−Py* interaction in **2**·Ca^{2+}, while it is not observed in **2**·Pb^{2+}.

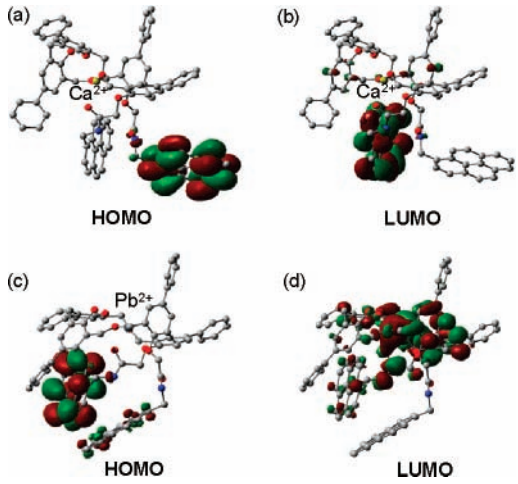

Figure 6. HOMO and LUMO for **2**·Ca^{2+} and **2**·Pb^{2+} are shown: (a) HOMO of **2**·Ca^{2+}, (b) LUMO of **2**·Ca^{2+}, (c) HOMO of **2**·Pb^{2+}, and (d) LUMO of **2**·Pb^{2+}.

In this regard, one can rationalize the fluorescence changes upon metal ion complexations that for the **2**·Ca^{2+} complex the eminent HOMO−LUMO interaction between Py and Py* become more efficient upon Ca^{2+} binding with the preferred geometry of allowing H-bonding between pyrenyl amide groups. In contrast, in the case of the **2**·Pb^{2+} complex, a tighter complex between Pb^{2+} and **2** is formed without H-bonding in pyrenyl amide moieties providing no Py−Py* interactions, in consequent, quenched excimer emissions as illustrated in Figure S7 (Supporting Information). It is also noted that the monomer and quenched excimer emission band in the fluorescence spectra of **2**·Pb^{2+} is attributed to the heavy metal quenching effect.

In summary, **1** and **2** were synthesized, and their conformations were confirmed by the ^1H and ^{13}C NMR spectra, which is in agreement with the theoretical calculation. On the basis of fluorescent spectra changes upon metal ion complexation, unlike **1**, **2** reveals that the binding of Ca^{2+} provides an enhanced excimer and declining monomer emission with ratiometric response. Upon Ca^{2+} binding, the efficient HOMO−LUMO interaction between Py and Py* induces a strong excimer emission band, whereas there is no such interaction observed upon Pb^{2+} complexation.

Acknowledgment. This research was supported by Grant of Korea Research Foundation [KRF-2004-015-C00303 (J. S. Kim) and KRF-2005-003-C00092 (S. Ham)].

Supporting Information Available: Additional figures and calculation data. This material is available free of charge via the Internet at http://pubs.acs.org.

OL0602396